Analysis and MPPT control of a wind-driven three-phase induction generator feeding single-phase utility grid

Krishnan Arthishri, Natarajan Kumaresan, Nanjappagounder Ammasaigounden

Department of Electrical and Electronics Engineering, National Institute of Technology, Tiruchirapalli, Tamil Nadu, India
E-mail: 407114006@nitt.edu

Published in *The Journal of Engineering*; Received on 9th March 2017; Accepted on 18th April 2017

Abstract: In this study, a three-phase diode bridge rectifier and a single-phase voltage source inverter topology has been proposed for feeding single-phase utility grid employing a three-phase induction generator fed from wind energy. A self-excited induction generator configuration has been chosen for wide speed operation of wind turbine system, which gives the scope for extracting maximum power available in the wind. In addition to maximum power point tracking (MPPT), the generator can be loaded to its rated capacity for feeding single-phase utility grid using a three-phase induction machine, whereas it is not possible with existing configurations because of the absence of power converters. For the proposed system, MPPT algorithm has been devised by continuously monitoring the grid current and a proportional resonant controller has been employed for grid synchronisation of voltage source inverter with single-phase grid. A MATLAB/Simulink model of the proposed system has been developed to ascertain its successful working by predetermining the overall performance characteristics. The present proposal has also been tested with sag, swell and distortion in the grid voltage. The control strategy has been implemented using field programmable gate array (FPGA) controller with modularised programming approach. The efficacy of the system has been demonstrated with the results obtained from an experimental set-up in the laboratory.

Nomenclature

v_{qs}, v_{ds}	stator q-axis and d-axis voltage, respectively, V
i_{qs}, i_{ds}	stator q-axis and d-axis current, respectively, A
v_{qr}, v_{dr}	rotor q-axis and d-axis voltage, respectively, V
i_{qr}, i_{dr}	rotor q-axis and d-axis current, respectively, A
φ_{qs}, φ_{ds}	stator q-axis and d-axis fluxes, respectively, Wb
φ_{qr}, φ_{dr}	rotor q-axis and d-axis fluxes, respectively, Wb
R_s, R_r	per phase stator and rotor resistance, respectively, Ω
L_s, L_r	total stator and rotor inductance, respectively, H
L_{ls}, L_{lr}	per phase stator and rotor leakage inductance, respectively, H
X_s, X_r	per phase stator and rotor leakage reactance, respectively, Ω
L_m	magnetising inductance, H
p	number of pole pairs
ω	reference frame angular velocity, rad/s
ω_r	electrical angular velocity, rad/s
ω_m	angular velocity of rotor, rad/s
T_m	shaft mechanical torque, Nm
T_e	electromagnetic torque, Nm
J	combined rotor and load inertia coefficient, kg m^2
H	combined rotor and load inertia constant
F	combined rotor and load viscous friction coefficient, Nm s/rad

1 Introduction

There has been a rising awareness worldwide to utilise renewable energy not only for addressing climate change due to environmental pollution, but also for providing access to the billions of people still living without electricity [1–4]. Owing to technological improvements and significant cost reductions, power generation from wind energy is nearly competitive with conventional fuels. Hence, wind energy electric conversion system plays a vital role for rural electrification to satisfy the electricity needs of the people living in remote locations. With financial and geographical constraints, it will be economical to install single-phase transmission lines in the initial stage of development to cater electricity to these remote locations. Squirrel-cage induction machine has been employed in commercial wind farms worldwide due to its ruggedness, almost nil maintenance, low cost and it does not require any synchronising equipment and additional dc source for its operation [3–9]. Use of standard three-phase squirrel-cage induction machine has been advocated with this single-phase system for ratings more than 3 kW because of its wide availability and lower cost as compared with single-phase induction machine [10–13]. Further, the same machine can be used without replacement or significant additional investment, if the transmission system is upgraded to three-phase at a later stage.

When the three-phase generator is configured to feed a single-phase grid, the unbalance between the three-phase currents should be reduced as much as possible. With a view to minimise this unbalance, various configurations as shown in Fig. 1 were proposed in the literature for feeding power to the single-phase grid employing three-phase induction machine [14–17]. In these configurations, the unbalance factor will vary with the operating slip and the minimum unbalance can be achieved only for a particular value of the operating slip. It has been reported that 80% of the rated power output of the machine capacity can be achieved when the machine is operated in the reverse direction with a single capacitor configuration for a slip of 3.1% [17]. Hence, the limitations of the configurations given in Fig. 1 are the underutilisation of machine capacity and the limited operating speed range of induction generator which is not suitable for maximum power extraction from wind energy. Few researchers have proposed induction generator for simultaneously feeding three-phase isolated loads and single-phase utility grid through power electronic converters [18–20]. In this arrangement, when the generated power is higher than the load demand, the excess power will be delivered to the single-phase utility grid and if the generated power is lower compared with the load demand, the single-phase utility grid will support the load. Further, this scheme has been proposed for those systems whose primary energy sources are micro-hydroelectric plants and diesel generator systems that operate with a narrow range of rotor speed variation. Bojoi *et al.* [21] have presented the commercial gasoline internal combustion engine driven single-phase grid connected system employing a three-phase induction machine and a back-to-back connected voltage source converter. A precise

This is an open access article published by the IET under the Creative Commons Attribution License (http://creativecommons.org/licenses/by/3.0/)

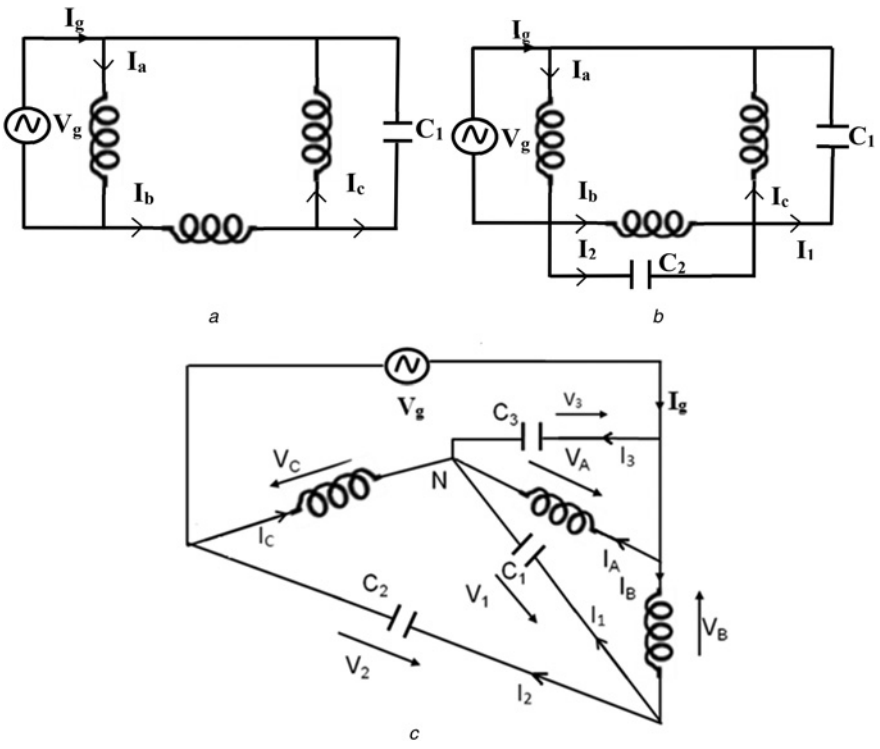


Fig. 1 *Stator winding configurations for three-phase induction generator supplying single-phase grid*
a Single capacitor configuration
b Two capacitor configuration
c Smith connection

configuration for the balanced operation of three-phase induction generator with maximum power point tracking (MPPT) feeding single-phase utility grid from wind energy is not available in the literature. Hence, an attempt is made in this paper to carry out a detailed analysis on the operation of three-phase induction generator along with the power electronic controllers feeding a single-phase utility grid suitable for rural electrification from wind energy.

In wind energy conversion system, the rotational speed of the WT should be allowed to vary with the wind velocity for MPPT [22–26]. Hence, for wide speed operation of the wind generator system, three-phase induction machine is operated in a self-excited mode and connected to the utility grid through power converters. The proposed system employs once such configuration for feeding power from three-phase self-excited induction generator (SEIG) to a single-phase utility grid using a three-phase diode bridge rectifier (DBR) and a single-phase voltage source inverter (VSI). The salient features of the proposed configuration for feeding single-phase grid are (i) balanced operation of the generator for all loads, (ii) the generator can be loaded till its rated capacity and (iii) possibility of maximum power extraction from the wind against the configurations shown in Fig. 1. Different MPPT algorithms have been proposed in the literature with and without speed sensors [22–32]. With mechanical speed sensors, the accuracy of tracking is less and the maintenance and operational costs are high. To overcome this difficulty, MPPT control algorithms are developed by sensing the electrical quantities namely the voltage and current [26, 28]. Adaptive MPPT is also gaining interest of the researchers due to the sensor-less behaviour of the tracking system [29–32]. However, this method includes high computations and training procedures. Hence, an attempt is made in this paper to develop a simple MPPT algorithm suitable for rural electrification feeding power to the single-phase utility grid. By taking advantage of the known single-phase grid voltage, in this paper, a MPPT algorithm has been developed by sensing only the current fed to the grid.

Grid synchronisation and control of the VSI play a vital role in the operation of the proposed system. In this regard, various strategies have been proposed in the literature for synchronising and controlling the VSI feeding power to the single-phase utility grid from renewable sources [33–37]. As compared with other controllers, proportional resonant (PR) controller has the advantages of selective harmonic compensation, better performance in tracking the grid reference and a reduced computational load [34, 35]. Hence, in this paper, PR control strategy with a linear current control scheme has been chosen for synchronisation and control of the grid tied VSI fed from wind energy.

The paper is organised as follows. The description of the proposed system along with the control strategy is explained in Section 2. Section 3 presents the system modelling and the performance analysis for both steady-state and dynamic conditions. Experimental investigations of the proposed system and the control scheme are given in Section 4. Conclusion is summarised in Section 5.

2 Description of the proposed system

The schematic diagram of the proposed wind energy conversion system for feeding single-phase utility grid is shown in Fig. 2. It comprises of a SEIG, a three- phase DBR, a single-phase VSI and filter components. The output voltage from the SEIG is of variable voltage-variable frequency (VV-VF) nature and the voltage and frequency values depend on the available wind energy and effective load at the generator terminals. The DBR converts this VV-VF ac voltage into a variable dc voltage. A single-phase VSI has been interfaced between the three-phase DBR and the single-phase utility grid through appropriate filters. The VSI is controlled in a closed loop for extracting the maximum power available in

This is an open access article published by the IET under the Creative Commons Attribution License (http://creativecommons.org/licenses/by/3.0/)

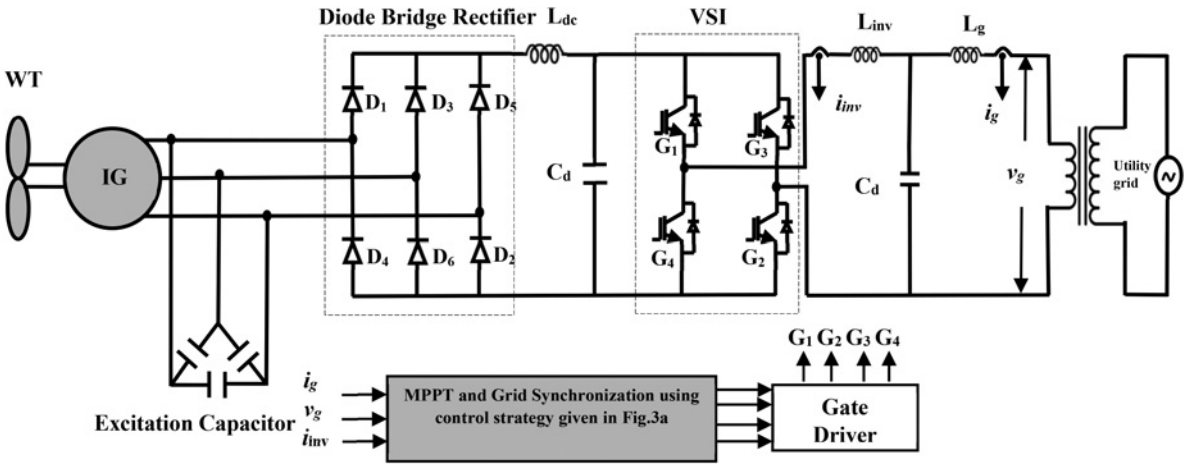


Fig. 2 *Schematic diagram of the proposed system for rural electrification from wind energy*

the wind with an acceptable grid current total harmonic distortion (THD) level (< 5%) and unity power factor (UPF) operation at the single-phase utility grid. For achieving this, a control strategy has been developed and the schematic diagram of the same is given in Fig. 3. This strategy has two major components namely (i) MPPT employing the P&O algorithm and (ii) current control and grid synchronisation using PR controller.

2.1 MPPT algorithm

In the proposed system, the grid current will vary for any variation in the output power from the wind-driven SEIG. This is due to the fact that (i) the grid voltage is constant and (ii) UPF is maintained at the grid side by appropriately controlling the VSI. Therefore, the MPPT algorithm has been developed by continuously monitoring the ac grid current employing the P&O algorithm as shown in Fig. 3*b*. This algorithm involves the comparison of the present and previous rms values of the ac grid current and based on the relative value of this comparison it gives the value of gain (k). This gain, k, is continuously adjusted in the closed loop by monitoring the ac grid current. By this algorithm the ac grid current is always maintained at a maximum possible value for extracting the maximum power available in the wind.

2.2 Current control and grid synchronisation

In the present work, PR controller structure given in [34] is implemented for the operation of the grid-tied VSI. This PR controller has a tracking regulator with the proportional gain K_p, a generalised integrator to resonate at the grid frequency, $H_1(s)$ and a harmonic compensator, $H_c(s)$ as shown in Fig. 3*a*. $H_1(s)$ and $H_c(s)$ are given below:

$$H_1(s) = \frac{K_i s}{s^2 + \omega_0^2} \tag{1}$$

where K_i is the fundamental integral gain, $\omega_0 = 2\pi f_0$ and f_0 is the grid frequency (50 Hz)

$$H_c(s) = \sum_{n=3}^{h} \frac{K_n s}{s^2 + (n\omega_0)^2} \tag{2}$$

where K_n is the nth harmonic integral gain and $n = 3,5,7,\ldots,h$, h being the highest component of harmonic current to be attenuated.

It is to be noted that the ideal PR controller described by (1) and (2) offers infinite gain at the respective resonant frequency. Hence, the practical realisation of an ideal PR controller is difficult and hence it is implemented as per the following modified equations [34, 35]:

$$H_1(s) = K_i \frac{2\xi\omega_0 s}{s^2 + 2\xi\omega_0 s + \omega_0^2} \tag{3}$$

$$H_1(s) = K_i \frac{2\xi\omega_0 s}{s^2 + 2\xi\omega_0 s + \omega_0^2} \tag{4}$$

where ξ is the damping factor.

For the current control and grid synchronisation of VSI, the grid voltage (v_g) and the inverter output current (i_{inv}) are sensed and given as inputs to the proposed closed-loop control scheme shown in Fig. 3*a*. The reference current signal (i_{ref}) is generated by multiplying the grid voltage, v_g with the gain, k obtained from the MPPT block. The reference current thus generated has two components, namely, the voltage reference for the grid synchronisation of VSI and the optimum value of grid current for maximum power extraction from wind. The reference signal for sinusoidal pulse width modulation (v_{pk}) is obtained from the PR controller using i_{ref} and i_{inv}. This signal is compared with the carrier signal (v_c) for generating pulses to control the insulated-gate bipolar transistors (IGBTs) in the VSI.

3 Analysis of the proposed system

To show the efficacy of the proposed system in feeding single-phase utility grid from wind energy source, both the steady-state and dynamic analyses have been carried out by building a MATLAB/Simulink model using the SimPowerSytems toolbox. This model has three major components namely a wind turbine (WT) model, a generator model and the power and control circuit models. Details on the development of these models/components are explained below.

3.1 WT model

For verifying the working of the proposed system feeding single-phase utility grid along with MPPT, the WT model available in the MATLAB is used as a prime mover for driving the generator. Mathematical modelling of the WT is widely available in the literature [22–32] and this model has been used for the simulation of the WT. The WT has been configured such that it gives a nominal mechanical power output of 5 kW for a base wind velocity of 12 m/s. The WT parameters used for the simulation are, maximum power at base wind velocity = 0.95 p.u.; base rotational speed = 1 p.u. (1500 rpm); gear ratio = 1:1; air density, $\rho = 1.205$ kg/m^3; power coefficient, $C_p(\max) = 0.48$ for the tip speed ratio, $\lambda = 8.1$ and the blade pitch angle, $\beta = 0°$.

This is an open access article published by the IET under the Creative Commons Attribution License (http://creativecommons.org/licenses/by/3.0/)

doi: 10.1049/joe.2017.0091

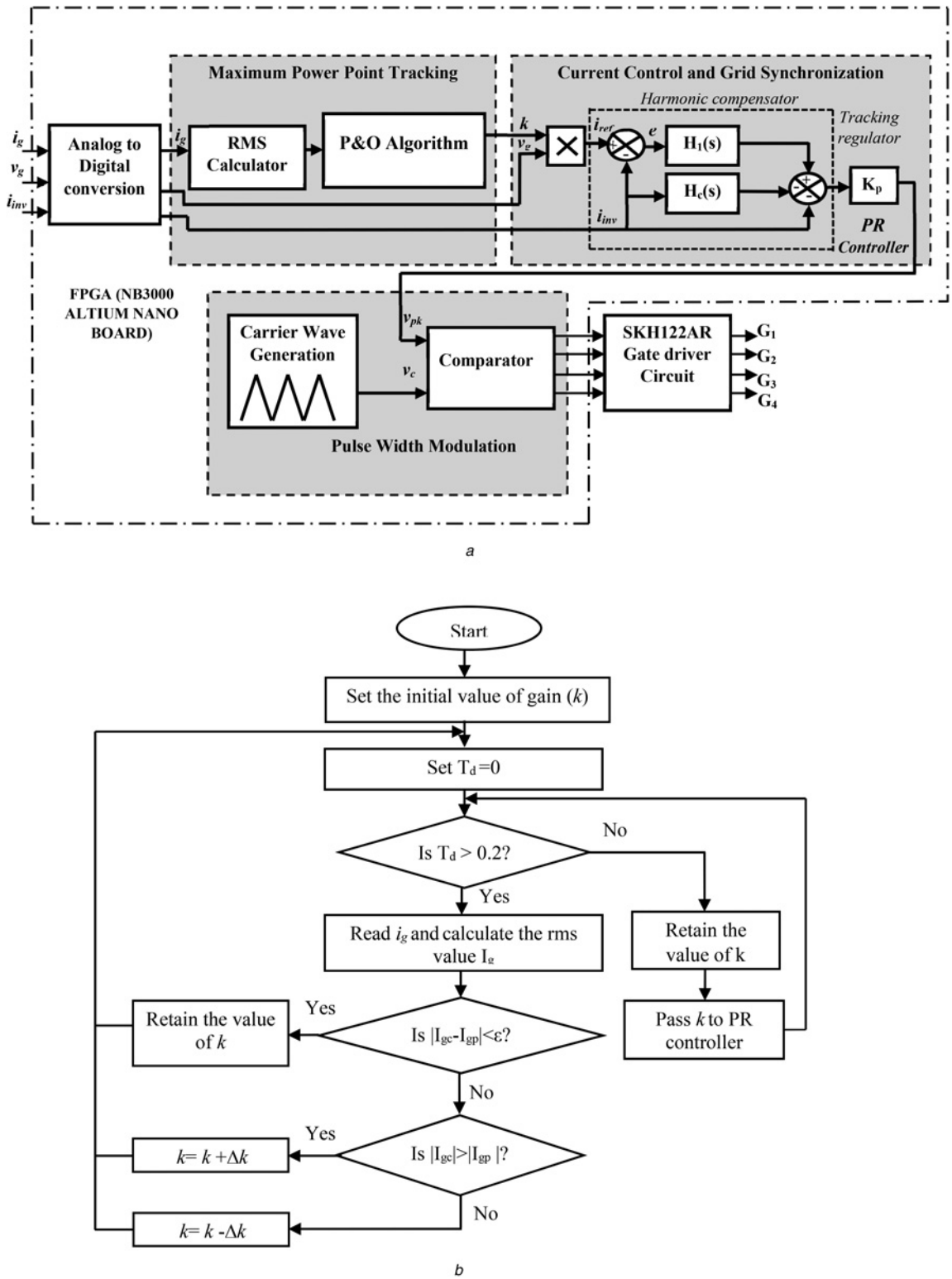


Fig. 3 *Proposed control strategy*
a Block diagram of the control technique
b Flowchart of the MPPT algorithm
T_d: time delay in seconds; i_g: grid current; I_{gc}: present value of the grid current; I_{gp}: previous value of the grid current; ε: tolerance which is taken as 0.001; k: gain; Δk: change in gain

3.2 Induction generator model

To show the working of the proposed system, a three-phase, four-pole, 230 V, 50 Hz, 3.7 kW, delta-connected squirrel-cage induction machine is operated as a SEIG with a capacitor of 100 µF per phase. This machine delivers rated power and rated voltage for a speed of 1500 rpm. Hence, the base rotational speed is taken as 1500 rpm for designing the WT for driving this SEIG. Experimentally obtained parameters of this induction machine are $R_s = 1.3\ \Omega$, $R_r = 1.75\ \Omega = 2.6\ \Omega$ and $X_s = X_r = 2.6\ \Omega$.

For analysing the proposed system, asynchronous machine model available in the MATLAB library is used. Dynamic

doi: 10.1049/joe.2017.0091
This is an open access article published by the IET under the Creative Commons Attribution License (http://creativecommons.org/licenses/by/3.0/)

Table 1 No-load saturation curve parameters of a three-phase, four-pole, 230 V, 3.7 kW, delta-connected induction machine

I_s, A	1.7	2.6	3.3	3.8	4.3	6.1	8.1	10.5	11.5	14.1	16.2	18.0
V_s, V	118	163	190	208	223	255	285	300	321	367	386	395

I_s is the stator current; V_s is the stator voltage; the first point (first column of the table) corresponds to the point where the effect of saturation begins.

modelling of the asynchronous machine is implemented using the following equations [38]:

$$V_{qs} = R_s i_{qs} + \omega\phi_{ds} + \rho\phi_{qs} \tag{5}$$

$$V_{ds} = R_s i_{ds} - \omega\phi_{qs} + \rho\phi_{ds} \tag{6}$$

$$V_{qr} = R_r i_{qr} + (\omega - \omega_r)\phi_{dr} + \rho\phi_{qr} \tag{7}$$

$$V_{dr} = r_r i_{dr} - (\omega - \omega_r)\phi_{qr} + \rho\phi_{dr} \tag{8}$$

$$T_e = 1.5p\left(\phi_{ds} i_{qs} - \phi_{qs} i_{ds}\right) \tag{9}$$

where

$$\rho = (d/\mathrm{d}t); \quad \omega_r = \omega \times p; \quad \phi_{qs} = L_s i_{qs} + L_m i_{qr};$$

$$\phi_{ds} = L_s i_{ds} + L_m i_{dr};$$

$$\phi_{qr'} = L_r i_{qr} + L_m i_{qs}; \quad \phi_{dr'} = L_r i_{dr} + L_m i_{qs}; \quad L_s = L_{ls} + L_m;$$

$$L_r = L_{lr} + L_m$$

The equations expressed in (5)–(9) are in a two axis (dq) reference frame. Iron loss component is ignored and the machine parameters are assumed to be constant in this modelling. The modelling of the mechanical system is given by

$$\rho\omega_m = \frac{1}{2H}\left(T_e - F\omega_m - T_m\right) \tag{10}$$

$$\rho\theta_m = \omega_m \tag{11}$$

The asynchronous machine model available in the MATLAB is configured to operate as an SCIG with torque as an input parameter. The negative value of the torque output from the WT model is given as the input to the machine to operate it as a generator. It is well known that the no-load saturation curve of an induction machine is a non-linear function and SEIG operates in the saturation region of the magnetisation characteristic [39]. Hence, it is required to give the no-load saturation curve points in the asynchronous machine model to operate it as a SEIG. The no-load saturation characteristic is specified as points in the machine model by a $2 \times n$ matrix, where n is the number of points taken from the saturation curve. The experimentally obtained no-load saturation characteristics for the three-phase, four-pole, 3.7 kW delta connected induction machine is given in Table 1. Further, the residual

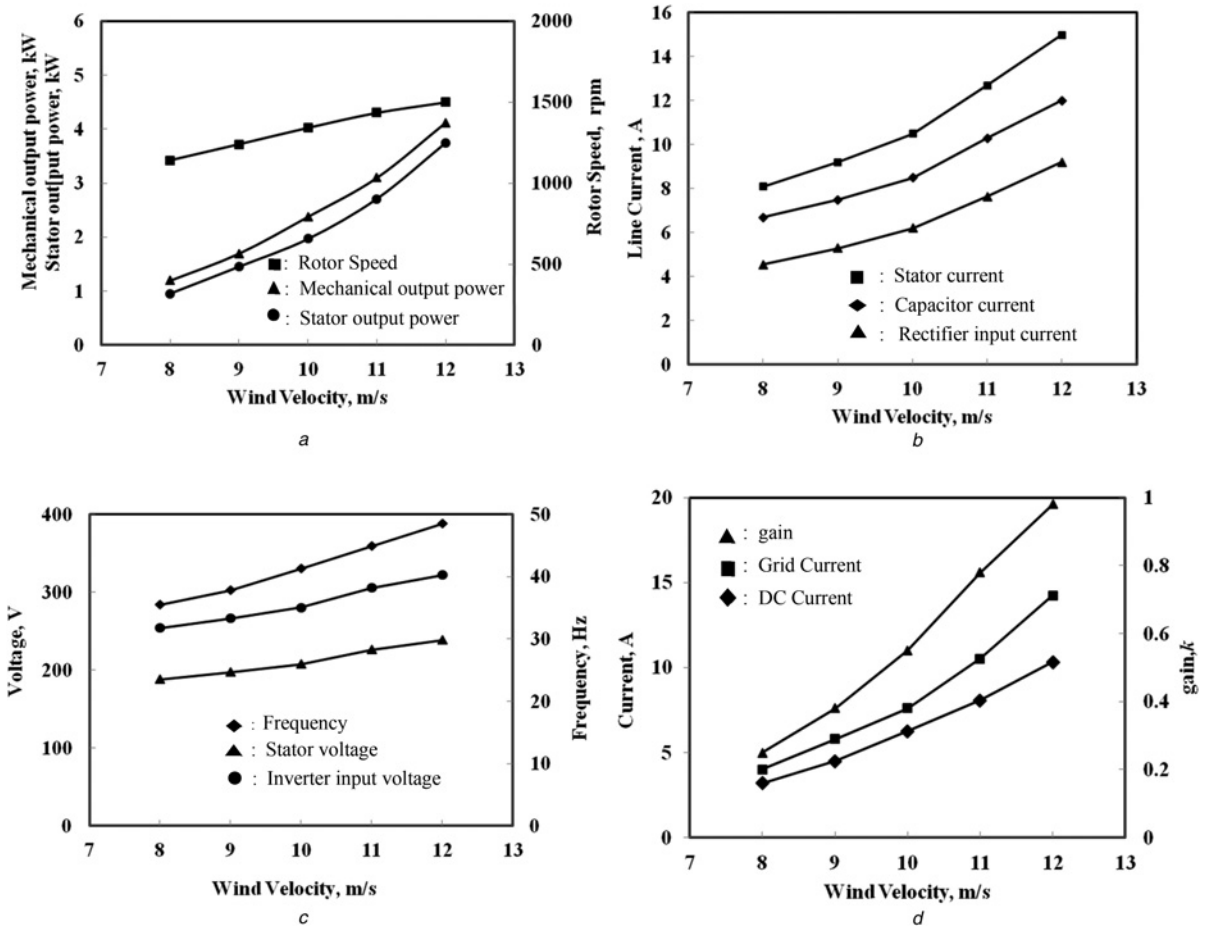


Fig. 4 *Steady-state response of the proposed system at MPPT condition for different wind velocities*
a Output power\rotor speed against wind velocity
b Voltage/frequency against wind velocity
c Line current against wind velocity
d Current\gain against wind velocity

This is an open access article published by the IET under the Creative Commons Attribution License (http://creativecommons.org/licenses/by/3.0/)

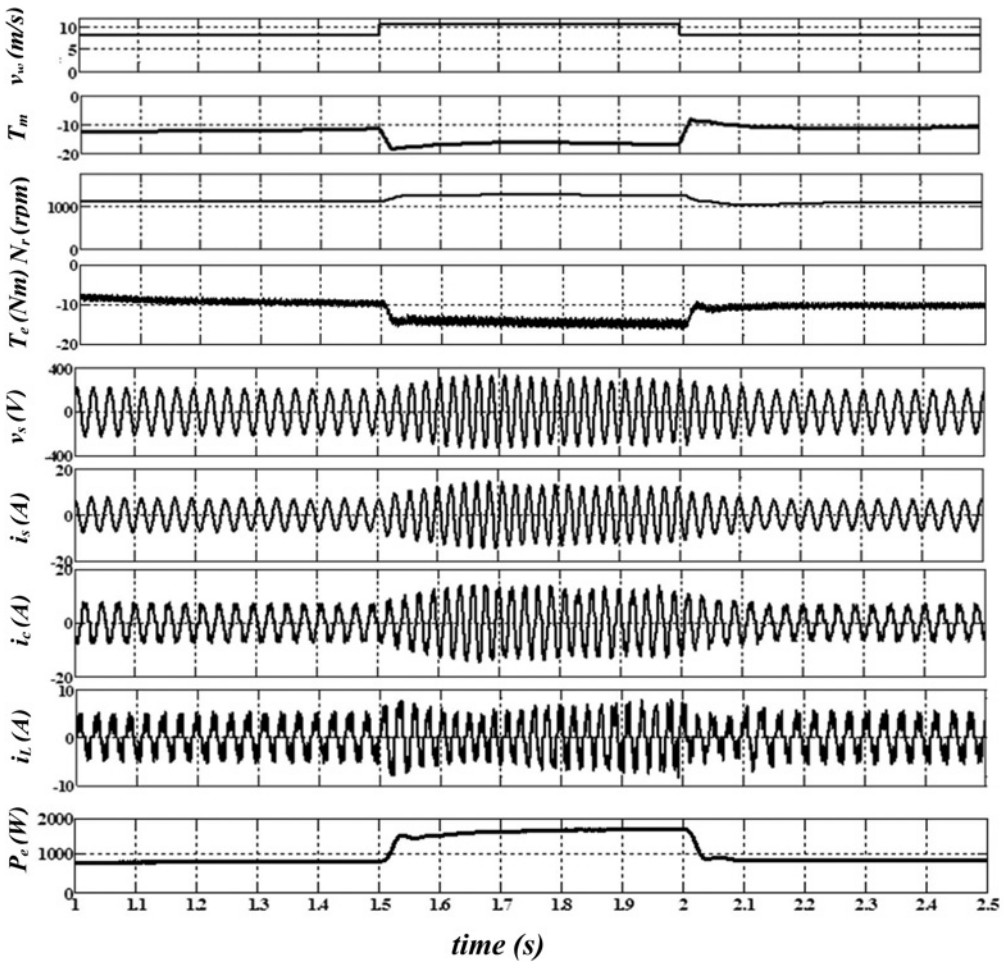


Fig. 5 *Dynamic response of WT and SEIG parameters for the step change in wind velocity*
v_w: wind velocity, T_m: mechanical torque, N_r: rotational speed, T_e: electromagnetic torque, v_s: stator voltage, i_s: stator current, i_c: capacitor current, i_l: rectifier input current, P_e: electrical power output from generator

flux should be present in the machine for the self-excitation and hence the initial stator currents are given in the machine model with finite values. To meet the reactive power requirement and also for self-excitation, a 100 μF/phase capacitor has been connected at the stator terminals of this machine model.

3.3 Power and control circuit

For the simulation study, the power circuits, namely, three-phase DBR and single-phase VSI are built using the diode and IGBT models available in the SimPowerSystems toolbox. The values of the filter components used in the simulation are: $L_{dc} = 10$ mH; $C_{dc} = 1000$ μF; $L_{inv} = 7$ mH; $L_g = 0.96$ mH; $C_g = 30$ μF; $R_d = 2.5$ Ω. The values of L_{dc} and C_{dc} have been chosen so that the dc voltage at the input terminal of VSI is ripple free and current at the dc terminal of the DBR is continuous. The grid side filter is designed so as to reduce the harmonics in the current fed to the grid [40]. The single-phase utility grid is realised using a single-phase voltage source available in the MATLAB.

The MPPT algorithm described in Section 2 has been implemented by writing the appropriate code in the embedded MATLAB function. The PR controller for the current control and grid synchronisation is realised using the transfer function block (s-function) available in the MATLAB. The values of PR controller parameters are: $\xi = 0.0001$; $K_p = 1$; $K_i = 10$; $K_3 = 70$; $K_5 = 70$. These values are selected by trial and error method in order to track the reference current and to maintain UPF at the utility grid. The output signal from the PR controller is taken as the reference signal, v_{pk} for the generation of PWM pulses. The triangular carrier wave, v_c of 5 kHz is compared with the reference signal, v_{pk} to generate the gating pulses to trigger the IGBTs of VSI.

3.4 Steady-state performance

The steady-state performance characteristics obtained from simulation for extracting the maximum power available from the wind are given in Fig. 4. Fig. 4*a* gives the maximum mechanical power output from the WT and the corresponding rotational speed for a given wind velocity. This figure also includes the electrical power output from the generator. It can be observed from this figure that the wind-generator system will operate for a specific value of rotational speed to extract maximum power from the wind. The dc input voltage to the VSI, stator voltage and the generated frequency of SEIG also vary with the wind velocity with the corresponding rotational speed for MPPT and the results are given in Fig. 4*b*.

The advantage of the proposed configuration is the balanced operation of currents in the three-phase machine as compared with a conventional system employing fixed phase balancing components for feeding a single-phase utility grid. This aspect is observed in the simulation and corresponding line currents at stator, capacitor and rectifier input terminals with respect to the wind velocity are given in Fig. 4*c*. As the balanced operation is achieved in the proposed configuration, the machine can be loaded till its rated capacity. This is seen from the electrical power output of the generator with respect to the wind velocity as given in Fig. 4*a*. Further, the generated frequency and the grid frequency are different in the proposed system as the machine terminals are decoupled from the single-phase utility grid employing power converters. This feature

This is an open access article published by the IET under the Creative Commons Attribution License (http://creativecommons.org/licenses/by/3.0/)

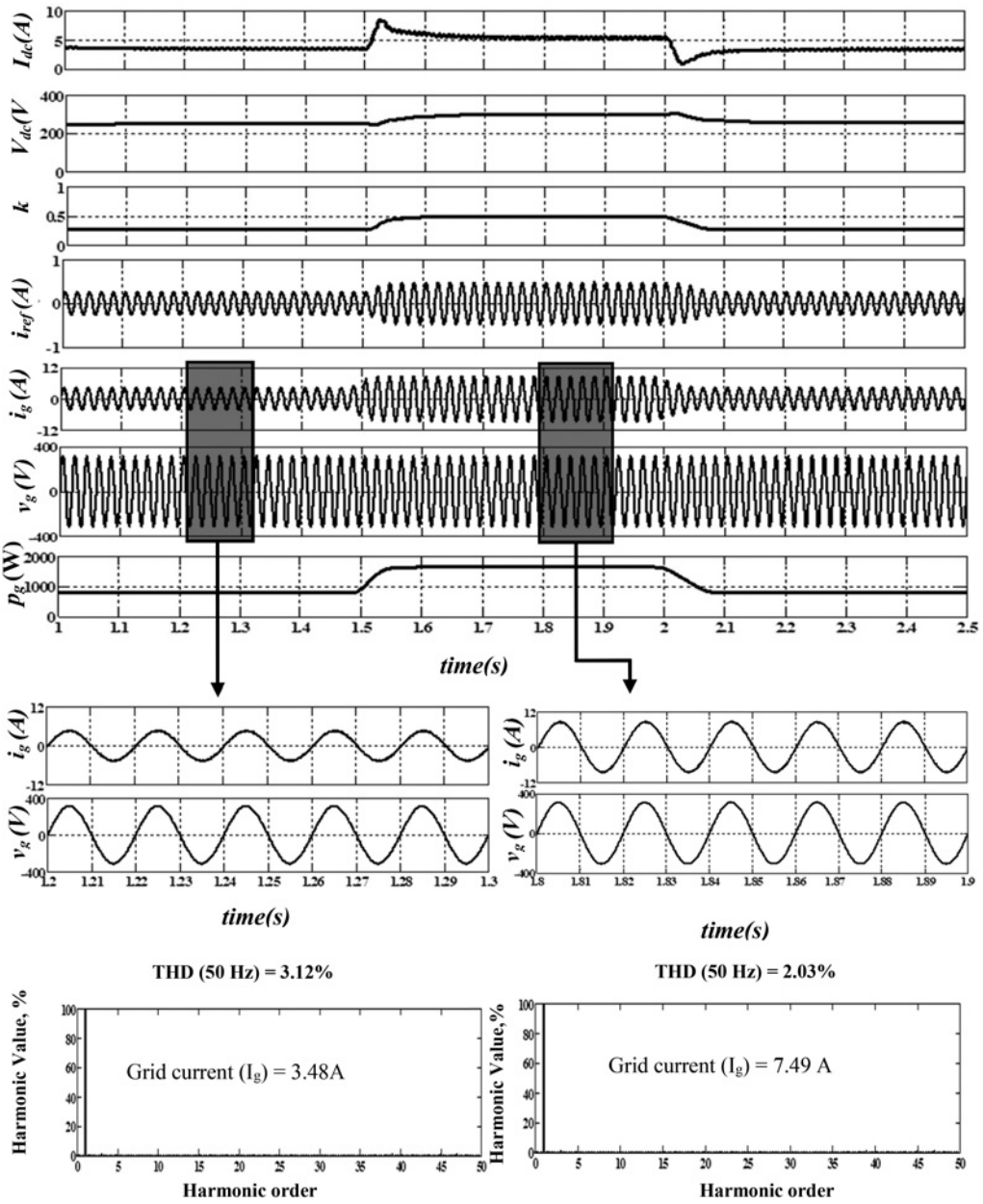


Fig. 6 *Dynamic response of the controller with dc and grid side performance quantities of 1-Φ VSI for a step change in wind velocity*
I_{dc}: inverter input current, V_{dc}: inverter input voltage, k: gain output from MPPT controller, i_{ref}: reference current to the PR controller, i_g: grid current, v_g: grid voltage, p_g: power fed to the grid

is essential for the wide speed operation of the induction generator to extract the maximum power available in the wind. Hence, the generator frequency will vary with the rotational speed and its variation with wind velocity is shown in Fig. 4*b*. Fig. 4*d* shows the variation of the gain and the corresponding grid current and dc input current to the VSI for maximum power extraction with wind velocity. This figure confirms that the proposed controller adjusts the gain with wind velocity for MPPT.

3.5 Dynamic performance

To verify the dynamic performance of the proposed system along with the control strategy, simulation has been carried out for various step changes in wind velocity. The response of the system for these conditions is observed in terms of the performance parameters of WT, SEIG, the intermediate power converter and the grid side parameters. For the sake of brevity, only the simulation results for a step change in the wind velocity from 8 to 10 m/s at $t = 1.5$ s and from 10 to 8 m/s at $t = 2$ s are given in Figs. 5 and 6. It can be observed from Fig. 5 that, for MPPT condition, there exists a particular rotor speed and a corresponding mechanical power output from the WT for a given wind velocity. As an example, at 8 m/s the rotational speed is 1135 rpm and the corresponding power output is 0.95 kW and these values are 1342 rpm and 1.85 kW, respectively, for 10 m/s. This figure also gives the corresponding variation of other performance quantities with respect to time for a step change in the wind velocity.

To illustrate the successful working of the proposed control strategy, the signals at various points of the controller shown in Fig. 3*a* were observed for various step changes in the wind velocity. Again for the sake of brevity, the simulated results are given in Fig. 6 for a change in wind velocity from 8 to 10 m/s and back. From this figure it can be noted that the controller adjust the gain, k by continuously monitoring the wind velocity for MPPT. This figure also shows the variation of dc voltage and current at the input side of VSI, grid voltage, grid current and harmonic spectra of the grid current. The enlarged view of the grid voltage and the grid current are also included in this figure to show the grid

This is an open access article published by the IET under the Creative Commons Attribution License (http://creativecommons.org/licenses/by/3.0/)

doi: 10.1049/joe.2017.0091

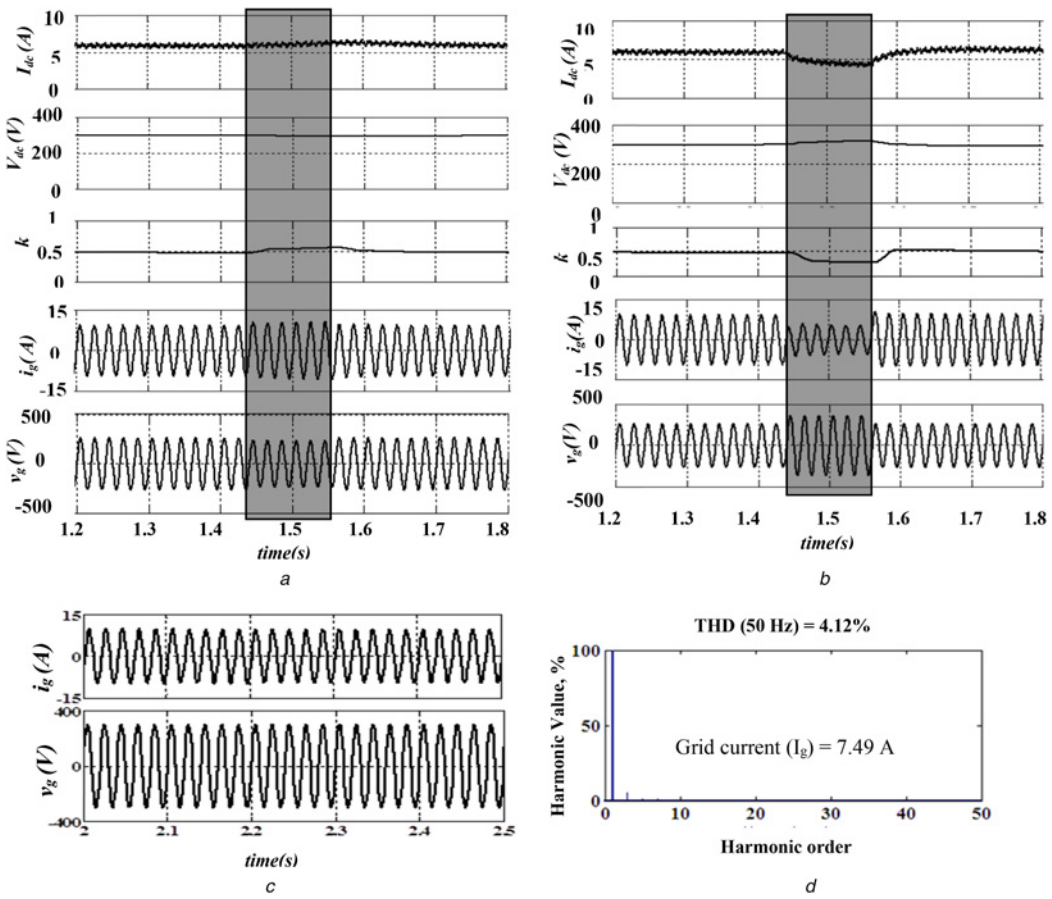


Fig. 7 *Response of the system with momentary disturbance and distortion in the grid voltage for a wind velocity of 10 m/s*
a Response of the system for 10% voltage sag
b Response of the system for 40% voltage swell
c Response of the system for a 10% THD in the grid voltage
d Harmonic spectra of the grid current with 10% THD in the grid voltage

synchronisation and UPF operation of the VSI employing the proposed control strategy. Further, it can be observed from the figure that proposed controller also maintains the grid current THD at lower than 5%. This exemplifies that the ac grid current is maintained close to sinusoidal by the proposed controller.

3.6 Response of the system with momentary disturbance and distortion in the grid voltage

In rural applications, one of the main problems is the poor power quality such as appreciable level of voltage variations and voltage distortion in the single-phase utility grid. As the proposed system is envisaged to be implemented with such systems, it is required to test the successful working of the proposed system for the momentary disturbances like sag, swell and distortion in the grid voltage. Hence simulation has been carried out for different conditions of voltage sag and swells in the grid. For the sake of brevity, the simulation results for a voltage sag of 10% and a voltage swell of 40% are given in Figs. 7*a* and *b*, respectively. For this simulation, the voltage sag and swell has been introduced at $t = 1.44$ s and maintained for six cycles. It can be observed from the simulated results that the gain k of the controller is adjusted according to the variation in the grid voltage and the normal operation of the system is restored after the momentary disturbance. Similarly, the distortion in terms of harmonics in the grid voltage is also considered to evaluate the performance of the system. Fig. 7*c* shows the grid side parameters for a grid voltage with a THD of 10%. The harmonic spectra of the grid current given in Fig. 7*d* shows that the grid current THD is maintained within the limit. This illustrates that the proposed control strategy feeds almost sinusoidal current even with the distorted grid voltage.

4 Experimental investigation

To demonstrate the working of the proposed system and the control strategy, a prototype was built in the laboratory. For this experimental study, the same three-phase, 230 V, 3.7 kW induction machine considered for the analysis in the previous section has been used. A separately-excited dc motor is used as a prime mover for driving the generator and for self-excitation, a capacitor bank of 100 μF/phase is connected at the stator terminals. A three-phase DBR module (MD8TU6012) has been used to convert the variable ac output voltage from SEIG into variable dc voltage. This variable dc voltage from DBR is given as the input to the single-phase VSI through a smoothing inductor and a dc link capacitor. A SEMIKRON make inverter module built using SKM100GB12V IGBTs along with the gate driver circuits is used as a single-phase inverter. The output of the single-phase inverter is connected to the single-phase 230 V, 50 Hz system through LC filter and an autotransformer. The values of the filter components and machine parameters are the same as used in the analysis.

The control strategy shown in Fig. 3*a* is implemented using a field programmable gate array (FPGA) (NB3000 Altium Nano Board) with SPARTAN 3AN package. The entire control strategy is implemented using a module-based Verilog coding for ADC, MPPT and PR control for current control and grid synchronisation. The grid voltage is sensed using LEM make voltage transducer (LV 25-P) and conditioned appropriately using signal conditioning

This is an open access article published by the IET under the Creative Commons Attribution License (http://creativecommons.org/licenses/by/3.0/)

Table 2 Performance of the proposed system for a given wind velocity

V_w, m/s	N_r, rpm	P_m, kW	sim/exp	V_S, V	I_S, A	I_C, A	I_L, A	f_g, Hz	P_e, kW	V_{dc}, V	I_{dc}, A	I_g, A
9	1220	1.7	sim	197.2	9.2	7.9	4.7	37.1	1.45	268.2	5.2	5.69
			exp	195.0	9.1	8.1	4.3	38.2	1.42	270.2	5.0	5.54
11	1440	3.2	sim	222.2	13.3	10.9	7.6	45.5	2.91	305.5	8.7	11.20
			exp	218.0	13.8	11.1	8.06	46.4	2.85	310.6	8.2	10.75

sim: results obtained from simulation, exp: results obtained from experiment; v_g: grid voltage (230 V).

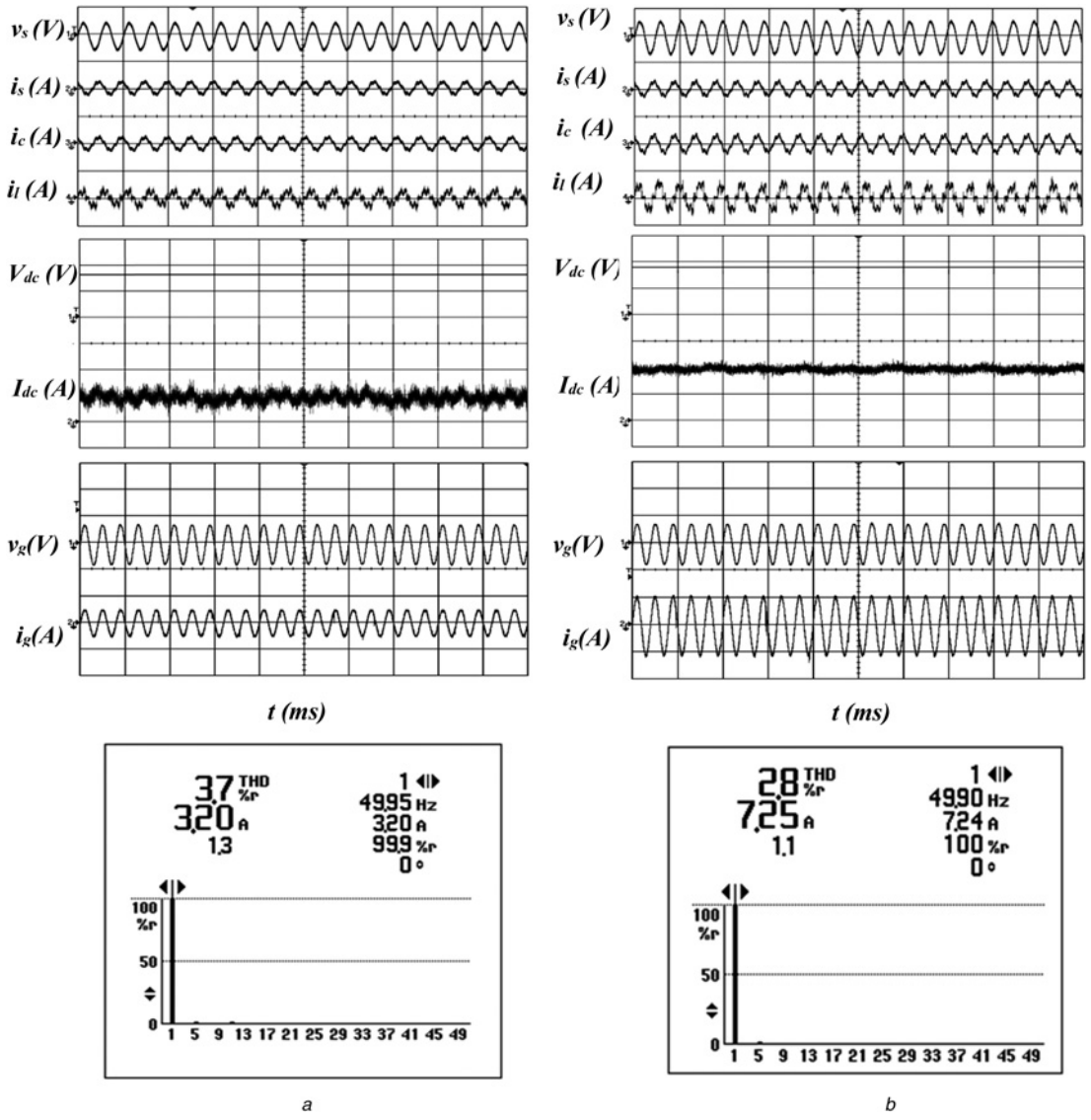


Fig. 8 *Experimental waveforms of the proposed system at MPPT condition*
v_s: stator voltage (500 V/div), i_s: stator current (50 A/div), i_c: capacitor current (50 A/div), i_l: rectifier input current (15 A/div), V_{dc}: dc voltage(150 V/div), I_{dc}: dc current (3 A/div), v_g: grid voltage (500 V/div), i_g: grid current (10 A/div), *t:* 50 ms/div
a At wind velocity of 8 m/s
b At wind velocity of 10 m/s

circuits before giving it to the FPGA board. Similarly, grid current and inverter currents are sensed using LEM make current transducer (LA-55) and given to FPGA board for closed-loop control. For digital implementation of PR control, the transfer functions given in (3) and (4) in *s*-domain are converted into *z*-domain by bilinear transformation (Tustin transformation) as given in [34, 35] which is

$$s = \frac{2}{T_s}\left(\frac{1 - z^{-1}}{1 + z^{-1}}\right) \tag{12}$$

where T_s is the sampling period. An up-down counter is used to generate the triangular carrier wave of 5 kHz internally. The gating pulses for IGBTs of VSI are generated by comparing the reference signal obtained from the PR control with the carrier wave.

To ascertain the working of the system, experiments have been conducted by setting a particular rotor speed and the MPPT controller gain to represent the maximum power point for a given wind velocity. These values are obtained from the simulation

This is an open access article published by the IET under the Creative Commons Attribution License (http://creativecommons.org/licenses/by/3.0/)

doi: 10.1049/joe.2017.0091

model described in Section 3 and the predetermined performance quantities are given in Table 2. For the sake of brevity, this table gives both the predetermined and experimental results for the wind velocities of 9 and 11 m/s.

The experimental waveforms of stator voltage, stator current, capacitor current and the input current to the DBR, dc voltage and current at the intermediate power converter stage and grid voltage and current, power fed to the grid were also observed using digital storage oscilloscope for different operating conditions. Fig. 8 shows these experimentally obtained results at MPPT condition for the wind velocities of 8 and 10 m/s and Figs. 5 and 6 show the corresponding waveforms obtained through simulations. It can be seen from these figures that the grid voltage and current are in-phase which validates the practical implementation of the proposed control strategy for the grid synchronisation and UPF operation of VSI. The grid current harmonic spectra were also experimentally captured using a harmonic analyser and the results are shown in Fig. 8. It can be noticed from this harmonic spectra that the current THD is lower than 5% which confirms the sinusoidal operation of the grid current employing the PR control. Closeness between the simulated and experimental results given in Table 2 and Figs. 5–8 validates the successful working of the control strategy developed for feeding a single-phase utility grid using the proposed wind-driven SEIG system.

To verify the working of the proposed system even with the momentary disturbance in the grid voltage, experiments have been conducted by introducing voltage sag and swell. For the experimental study, the machine has been rotated with a speed of 1342 rpm which corresponds to the MPPT condition for a wind velocity of 10 m/s. The grid voltage is varied for a short duration of time with the help of an auto-transformer and the voltage and current response at 110 V side are given in Fig. 9. It can be seen from this figure that, the grid current is adjusted by the controller by varying the gain according to the change in the grid voltage. These results further confirm the successful working of the proposed system even with momentary voltage fluctuations in the grid side.

5 Conclusion

The suitability of the wind-driven SEIG system with DBR and VSI for feeding single-phase utility has been studied. As the three-phase DBR is connected at the generator terminals, the SEIG supplies balanced load currents. This makes the operation of SEIG to its full rated capacity as compared with existing configurations using fixed phase balancing components. In this system, stator terminals of the generator are decoupled from the single-phase utility grid and hence the operating frequency of the SEIG is not same as that of the grid frequency. This allows the rotational speed of the wind-generator system to vary with wind velocity for extracting maximum power. For MPPT, a simple P&O based algorithm has been developed which requires continuous monitoring of the grid current. A closed-loop controller employing PR control has been developed and implemented for sinusoidal grid current, grid synchronisation and UPF operation.

To analyse the steady-state and dynamic performance of the proposed system along with the controller, a MATLAB/Simulink model has been developed. The asynchronous machine model available in the MATLAB library is suitably configured to operate as an induction generator and the configuration procedure is discussed in detail. Results obtained from the analysis show that the proposed system always tracks the maximum power available in the wind with balanced operation of induction generator and sinusoidal ac grid current. In order to validate the performance of the proposed system for practical implementation, a prototype was built in the laboratory and tested for various operating conditions. The closeness between the experimental and simulation results confirms the usefulness and successful working of the proposed system. The satisfactory response of the system has been observed both in simulation and experimentation for momentary disturbance in the grid voltage.

In summary, the attractive features of the proposed wind energy conversion system are (i) balanced operation of the generator phase currents leading to the utilisation of the generator to its rated capacity, (ii) simple power converter configuration, (iii) maximum

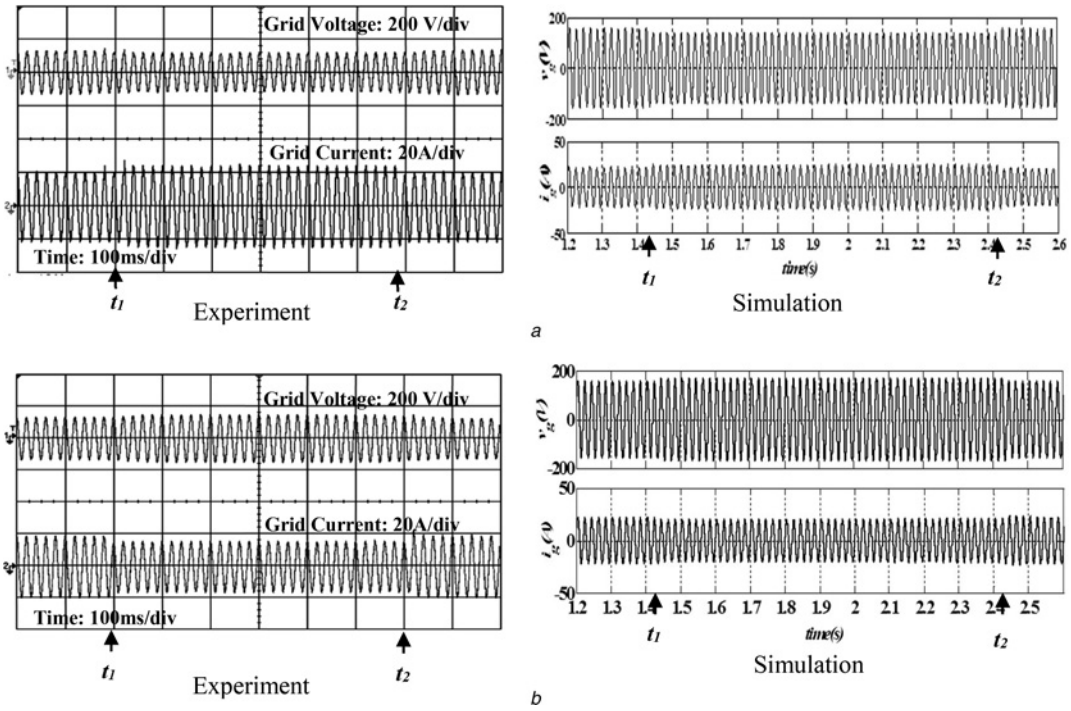


Fig. 9 *Experimental results with momentary distortion in the grid voltage*
t_1: instant at which voltage sag/swell is introduced; t_2: instant at which nominal voltage is restored
a Response of the system for a 10% voltage sag
b Response of the system for a 10% voltage swell

This is an open access article published by the IET under the Creative Commons Attribution License (http://creativecommons.org/licenses/by/3.0/)

power extraction from wind and (iv) very low current THD at the grid side. The proposed configuration will play a significant role in rural electrification, since single-phase utility grid is envisaged in the initial stages of development in the remote areas. Added feature of this configuration is that it requires only one additional leg in the VSI when the utility grid is upgraded to the three-phase system in the later stage. Hence, the proposed system is economical and cost effective for powering rural areas from wind energy.

6 References

[1] 'Renewables 2016 – global status report'. Available at http://www.ren21.net/status-of-renewables/global-status-report, 2016

[2] Kanase-Patil A.B., Saini R.P., Sharma M.P.: 'Integrated renewable energy systems for off grid rural electrification of remote area', *Renew. Energy*, 2010, **35**, (6), pp. 1342–1349, doi: http://dx.doi.org/10.1016/j.renene.2009.10.005

[3] Blaabjerg F., Ma K.: 'Future on power electronics for wind turbine systems', *IEEE J. Emerg. Sel. Top. Power Electron.*, 2013, **1**, (3), pp. 139–152, doi: 10.1109/JESTPE.2013.2275978

[4] Polinder H., Ferreira J.A., Jensen B.B., *ET AL.*: 'Trends in wind turbine generator systems', *IEEE J. Emerg. Sel. Top. Power Electron.*, 2013, **3**, (1), pp. 174–185, doi: 10.1109/JESTPE.2013.2280428

[5] Senthil Kumar S., Kumaresan N., Subbiah M.: 'Analysis and control of capacitor-excited induction generators connected to a micro-grid through power electronic converters', *IET Gener. Transm. Distrib.*, 2015, **9**, (10), pp. 911–920, doi: 10.1049/iet-gtd.2014.0529

[6] Simões M.G., Felix A.F.: 'Modeling and analysis with induction generators' (CRC Press, 2014, 3rd edn.)

[7] Bansal R.C.: 'Three-phase self-excited induction generators: an overview', *IEEE Trans. Energy Convers.*, 2005, **20**, (2), pp. 292–299, doi: 10.1109/TEC.2004.842395

[8] Kumaresan N., Subbiah M.: 'Innovative reactive power saving in wind-driven grid-connected induction generators using a delta-star stator winding: part II, estimation of annual Wh and VARh of the delta-star generator and comparison with alternative schemes', *Int. J. Wind Eng.*, 2003, **27**, (3), pp. 195–204, doi: https://doi.org/10.1260/030952403769016672

[9] Senthil Kumar S., Kumaresan N., Ammasai Gounden N., *ET AL.*: 'Analysis and control of wind-driven self-excited induction generators connected to the grid through power converters', *Front. Energy*, 2012, **6**, (4), pp. 403–412, doi: 10.1007/s11708-012-0208-8

[10] Ion C.P., Marinescu C.: 'Three-phase induction generators for single-phase power generation: an overview', *Renew. Sustain. Energy Rev.*, 2013, **22**, pp. 73–80, doi: http://dx.doi.org/10.1016/j.rser.2013.01.031

[11] Singh G.: 'Self-excited induction generator research – a survey', *Electr. Power Syst. Res.*, 2004, **69**, (2), pp. 107–114, doi: http://dx.doi.org/10.1016/j.epsr.2003.08.004

[12] Chan T.F., Lai L.: 'Three-phase induction generator operating on a single-phase power system'. IEEE Power Engineering Society General Meeting, Montreal, Que., 2006, pp. 1–4, doi: 10.1109/PES.2006.1709348

[13] Bansal R.C., Bhatti T.S., Kothari D.P.: 'Bibliography on the application of induction generators in nonconventional energy systems', *IEEE Trans. Energy Convers.*, 2003, **18**, (3), pp. 433–439, doi: 10.1109/TEC.2003.815856

[14] Chan T.F., Lai L.L.: 'Single-phase operation of a three-phase induction generator with the smith connection', *IEEE Trans. Energy Convers.*, 2002, **17**, (1), pp. 47–54, doi: 10.1109/60.986436

[15] Chan T.F., Lai L.L., Yan L.T.: 'Finite element analysis of a single-phase grid-connected induction generator with the steinmetz connection', *IEEE Trans. Energy Convers.*, 2003, **18**, (2), pp. 321–329, doi: 10.1109/TEC.2003.811737

[16] Chan T.F., Lai L.L.: 'Single-phase operation of a three-phase induction generator using a novel line current injection method', *IEEE Trans. Energy Convers.*, 2005, **20**, (2), pp. 308–315, doi: 10.1109/IEMDC.2003.1210315

[17] Chan T.F.: 'Performance analysis of a three-phase induction generator connected to a single-phase power system', *IEEE Trans. Energy Convers.*, 1998, **13**, (3), pp. 205–213, doi: 10.1109/60.707597

[18] Marra E.G., Pomilio J.A.: 'Induction-generator-based system providing regulated voltage with constant frequency', *IEEE Trans. Ind. Electron.*, 2000, **47**, (4), pp. 908–914, doi: 10.1109/41.857971

[19] Machado R.Q., Pomilio J.A., Marra E.G.: 'Electronically controlled bi-directional connection of induction generator with a single-phase grid'. The 27th Annual Conf. of the IEEE Industrial Electronics Society, 2001, pp. 1982–1987, doi: 10.1109/IECON.2001.975595

[20] Machado R.Q., Buso S., Pomilio J.A., *ET AL.*: 'Three-phase to single-phase direct connection rural cogeneration systems'. Applied Power Electronics Conf. and Exposition, 2004, pp. 1547–1553, doi: 10.1109/APEC.2004.1296070

[21] Bojoi R., Roiu D., Griva G., *ET AL.*: 'Single-phase grid-connected distributed generation system with maximum power tracking'. Int. Conf. on Optimization of Electrical and Electronic Equipment (OPTIM), May 2010, pp. 1131–1137, doi: 10.1109/OPTIM.2010.5510331

[22] Mesemanolis A., Mademlis C., Kioskeridis I.: 'Optimal efficiency control strategy in wind energy conversion system with induction generator', *IEEE J. Emerg. Sel. Top. Power Electron.*, 2013, **1**, (4), pp. 238–246, doi: 10.1109/JESTPE.2013.2284562

[23] Nayanar V., Kumaresan N., Gounden N.A.: 'A single-sensor-based MPPT controller for wind-driven induction generators supplying dc microgrid', *IEEE Trans. Power Electron.*, 2016, **31**, (2), pp. 1161–1172, doi: 10.1109/TPEL.2015.2420568

[24] Abdullah M., Yatim A., Tan C., *ET AL.*: 'A review of maximum power point tracking algorithms for wind energy systems', *Renew. Sustain. Energy Rev.*, 2012, **16**, (5), pp. 3220–3227, doi: http://dx.doi.org/10.1016/j.rser.2012.02.016

[25] Agarwal V., Aggarwal R.K., Patidar P., *ET AL.*: 'A novel scheme for rapid tracking of maximum power point in wind energy generation systems', *IEEE Trans. Energy Convers.*, 2010, **25**, (1), pp. 228–236, doi: 10.1109/TEC.2009.2032613

[26] Vijayakumar K., Kumaresan N., Ammasaigounden N.: 'Speed sensor-less maximum power point tracking and constant output power operation of wind-driven wound rotor induction generators', *IET Power Electron.*, 2015, **8**, (1), pp. 33–46, doi: 10.1049/iet-pel.2013.0700

[27] Linus R.M., Damodharan P.: 'Maximum power point tracking method using a modified perturb and observe algorithm for grid connected wind energy conversion systems', *IET Renew. Power Gener.*, 2015, **9**, (6), pp. 682–689, doi: 10.1049/iet-rpg.2014.0070

[28] Dalala Z.M., Zahid Z.U., Lai J.S.: 'New overall control strategy for small-scale WECS in MPPT and stall regions with mode transfer control', *IEEE Trans. Energy Convers.*, 2013, **28**, (4), pp. 1082–1092, doi: 10.1109/TEC.2013.2287212

[29] Kazmi S.M.R., Goto H., Guo H.J., *ET AL.*: 'A novel algorithm for fast and efficient speed-sensorless maximum power point tracking in wind energy conversion systems', *IEEE Trans. Ind. Electron.*, 2011, **58**, (1), pp. 29–36, doi: 10.1109/TIE.2010.2044732

[30] Benadja M., Chandra A.: 'Adaptive sensorless control of PMSG based offshore wind farm and VSC-HVDC stations', *IEEE J. Emerg. Sel. Top. Power Electron.*, 2015, **3**, (4), pp. 918–931, doi: 10.1109/JESTPE.2015.2453113

[31] Pucci M., Cirrincione M.: 'Neural MPPT control of wind generators with induction machines without speed sensors', *IEEE Trans. Ind. Electron.*, 2011, **58**, (1), pp. 37–47, doi: 10.1109/TIE.2010.2043043

[32] Wei C., Zhang Z., Qiao W., *ET AL.*: 'Reinforcement-learning-based intelligent maximum power point tracking control for wind energy conversion systems', *IEEE Trans. Ind. Electron.*, 2015, **62**, (10), pp. 6360–6370, doi: 10.1109/TIE.2015.2420792

[33] Teodorescu R., Blaabjerg F., Liserre M., *ET AL.*: 'Proportional-resonant controllers and filters for grid-connected voltage-source converters', *IEE Proc., Electr. Power Appl.*, 2006, **153**, (5), pp. 750–762, doi: 10.1049/ip-epa:20060008

[34] Castilla M., Miret J., Matas J., *ET AL.*: 'Linear current control scheme with series resonant harmonic compensator for single-phase grid-connected photovoltaic inverters', *IEEE Trans. Ind. Electron.*, 2008, **55**, (7), pp. 2724–2733, doi: 10.1109/TIE.2008.920585

[35] Yepes A.G.: 'Digital resonant current controllers for voltage source converters'. PhD thesis, University of Vigo, 2011

[36] Pandit J.K., Sakthisudhursun B., Aware M.V.: 'PR controller implementation using double update mode digital PWM for grid connected inverter'. IEEE Int. Conf. on Power Electronics, Drives and Energy Systems (PEDES), 2014, pp. 1–6

[37] Wu F., Zhang L., Wu Q.: 'Simple unipolar maximum switching frequency limited hysteresis current control for grid-connected inverter', *IET Power Electron.*, 2014, **7**, (4), pp. 933–945, doi: 10.1049/iet-pel.2013.0284

[38] Krause P., Wasynczuk O., Sudho S.: 'Analysis of electric machinery' (IEEE Press, 2002, 2nd edn.)

This is an open access article published by the IET under the Creative Commons Attribution License (http://creativecommons.org/licenses/by/3.0/)

[39] Ammasaigounden N., Subbiah M., Krishnamurthy M.R.: 'Wind-driven self-excited pole-changing induction generators', *IEE Proc. Electr. Power Appl.*, 1986, **133**, (5), pp. 315–321, doi: 10.1049/ip-b.1986.0042

[40] Reznik A., Simoes M.G., Al-Durra A., *ET AL.*: 'LCL filter design and performance analysis for grid-interconnected systems', *IEEE Trans. Ind. Appl.*, 2014, **50**, (2), pp. 1225–1231, doi: 10.1109/TIA.2013.2274612

This is an open access article published by the IET under the Creative Commons Attribution License (http://creativecommons.org/licenses/by/3.0/)